Minor salivary gland intraductal mucoepidermoid carcinoma: a case report

Ibrahim Nawroz, MBChB, FRCPath, DipFM,[a,1] Jonathan Bowman, BDS, MBChB, MFDS RCSEd,[b,1] Neil Frazer, BDS, FDS RCPS(Glasg),[b] and Victoria Cook, BDS, MBChB, MFDS RCPS(Glasg), MRCS Dip Trauma Surgery, FRCSEd(OMFS)[b]

We describe a case of an intraductal mucoepidermoid carcinoma arising from a minor salivary gland of the oral cavity. This is a rare presentation, and our literature review identified only a single previously documented case. To the best of our knowledge, this is the first reported case to be verified by immunohistochemistry demonstrating myoepithelial or basal cells around all the neoplastic units. (Oral Surg Oral Med Oral Pathol Oral Radiol 2019;128:e13–e15)

Minor salivary gland neoplasms comprise a diverse group of lesions that vary widely in their presentations and morphologies. Mucoepidermoid carcinoma is a malignant glandular neoplasm characterized by the presence of epidermoid cells, intermediate cells, and mucus-secreting cells. Here, we report the case of an intraductal mucoepidermoid carcinoma arising from a minor salivary gland of the oral cavity. A MEDLINE literature search identified only a single previously documented case in correspondence.[1] To the best of our knowledge, this is only the second reported case and the first to be supported by immunohistochemistry that demonstrated myoepithelial or basal cells around all the neoplastic units.

CASE REPORT

A 56-year-old female was referred to our department with a two-year history of a slow-growing painless lump to her right buccal mucosa. Her medical history was unremarkable. Clinical examination showed a solitary circumscribed 10×10 mm submucosal lesion, with a subtle blue hue, located immediately anterior to the orifice of Stenson's duct. Clinical appearances were thought to be consistent with a benign salivary mucocele, and the patient underwent carbon dioxide laser excisional biopsy under local anesthesia.

In view of unexpected histopathology results, a contrast-enhanced staging computed tomography scan was requested; however, this demonstrated no evidence of invasive or metastatic disease. Further limited resectional surgery under local anesthesia demonstrated no residual tumor. There was no recurrence at four-year follow-up, and the patient continues to undergo long-term review.

Histologic and Immunohistochemical Staining

Four formalin-fixed, paraffin-embedded tissue sections were stained with hematoxylin and eosin (H&E), Alcian blue, and periodic acid–Schiff (PAS) for routine histologic review. Further immunohistochemical staining was performed on formalin-fixed, paraffin-embedded tissue sections with use of antibodies against cytokeratin 5/6 (CK5/6), cytokeratin 7 (CK7), 34βE12, epithelial membrane antigen (EMA), cytokeratin 4 (EP4), MIB1, p53, p63, S100, smooth muscle actin (SMA), and vimentin (Table I).

RESULTS

Histopathology revealed parakeratotic buccal mucosa and underlying submucosa, including a minor salivary gland excretory duct. A 5mm intraluminal solid tumor occupied approximately 75% of the cystically enlarged duct lumen and was confluent with the ductal lining epithelium (Figure 1A). The tumor was predominately composed of uniform polyhedral clear cells, leading to peripheral islands of intermediate cells accompanied by mucinous goblet cells (Figures 1B–1E).

The tumor cells demonstrated no significant nuclear pleomorphism, no necrosis, and no obvious mitotic activity. There was a low MIB1 proliferative index of 2% to 3% in the most active foci within the intermediate cell component (Figure 2A). Diffuse positivity for 34βE12, CK7, and EP4 and widespread positivity for EMA and vimentin were seen (Figures 2B and 2C). There was no p53 overexpression. Immunochemistry for p63, CK5/6, and S100 confirmed no tumor extension beyond the duct basal layer (Figures 2D and 2E). The underlying minor salivary glands showed mild chronic inflammation with focal atrophy. There was no perineural or lymphovascular invasion, and the tumor was narrowly excised by 0.22 mm radially and 1.08 mm deep.

The tumor reported had all the morphologic attributes of an intraductal mucoepidermoid carcinoma. It was deemed histologically low grade on the basis of

[a]Department of Pathology, Victoria Hospital, Kirkcaldy, United Kingdom.
[b]Department of Oral and Maxillofacial Surgery, Victoria Hospital, Kirkcaldy, United Kingdom.
Received for publication Jul 27, 2017; returned for revision Feb 8, 2019; accepted for publication Feb 20, 2019.

2212-4403/$-see front matter
https://doi.org/10.1016/j.oooo.2019.02.018
[1]These authors contributed equally.

Table I. Immunohistochemical stains

Stain	*Clone*	*Manufacturer*	*Dilution*
CK5/6	Monoclonal mouse D5/16B4	Roche	Prediluted
CK7	Monoclonal rabbit SP52	Roche	Prediluted
34βE12	Monoclonal mouse 34βE12	Dako	1:100
EMA	Monoclonal mouse E29	Roche	Prediluted
EP4	Monoclonal rabbit EP4	Cell Marque	Prediluted
MIB1	Monoclonal rabbit 30-9	Roche	Prediluted
p53	Monoclonal mouse DO-7	Roche	Prediluted
p63	Monoclonal mouse 4A4	Roche	Prediluted
S100	Polyclonal rabbit anti-S100	Dako	1:8000
SMA	Monoclonal mouse 1A4	Roche	Prediluted
Vimentin	Monoclonal mouse V9	Roche	Prediluted

parameters including limited cytologic atypia and low mitotic activity. The presence of an infiltrative invasive component was excluded by thorough sampling and, further to the previously reported case, was confirmed by immunohistochemistry demonstrating preservation of pre-existing myoepithelial cells around the neoplastic units.

DISCUSSION

It is important to differentiate this rare neoplasm from other ductal carcinomas because misdiagnosis has significant therapeutic and prognostic implications. The principal differential diagnoses considered included mucoepidermoid carcinoma, salivary duct carcinoma in situ, clear cell adenocarcinoma, and epithelial−myoepithelial carcinoma.

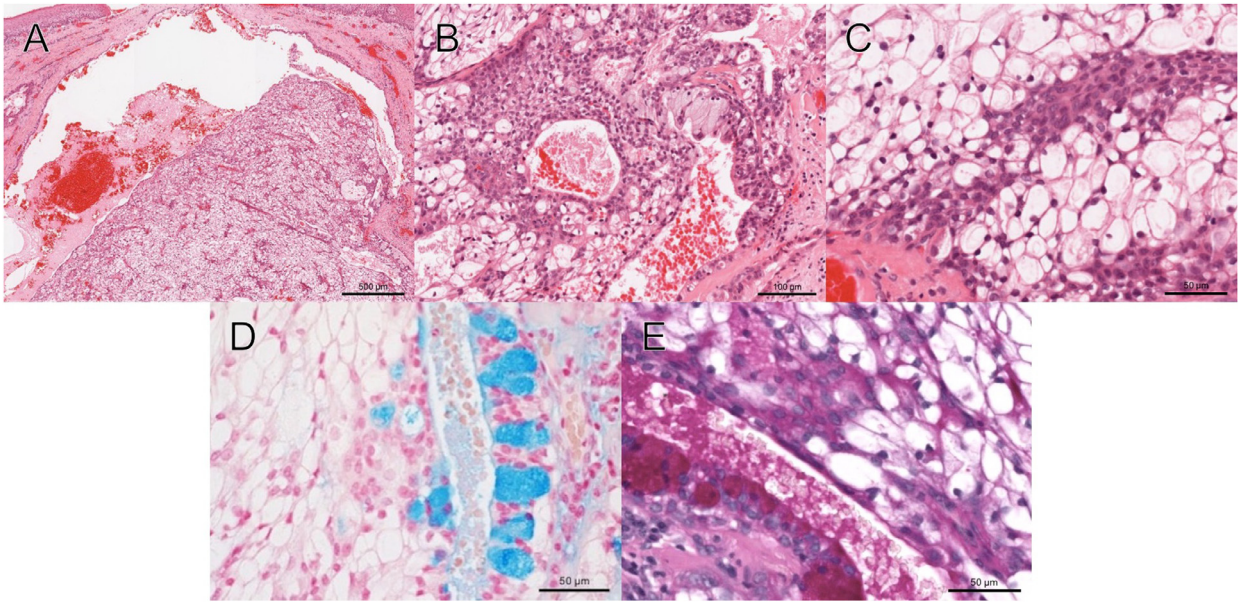

Fig. 1. **(A)** Intraductal solid tumor nodule (H&E; magnification as illustrated). *A high-resolution version of this slide for use with the Virtual Microscope is available as eSlide: VM05196.* **(B)** Predominant central polyhedral clear cells leading to peripherally situated intermediate and mucinous glandular cells (H&E; magnification as illustrated). *A high-resolution version of this slide for use with the Virtual Microscope is available as eSlide: VM05198.* **(C)** Dominant polyhedral tumor cells leading to a central area of intermediate tumor cells (H&E; magnification as illustrated). *A high-resolution version of this slide for use with the Virtual Microscope is available as eSlide: VM05198.* **(D)** Alcian blue highlighting mucinous goblet cells (Alcian blue; magnification as illustrated). *A high-resolution version of this slide for use with the Virtual Microscope is available as eSlide: VM05195.* **(E)** PAS highlighting mucinous goblet cells in the glandular element and glycogen granules in the clear cells (PAS; magnification as illustrated). *A high-resolution version of this slide for use with the Virtual Microscope is available as eSlide: VM05194.*

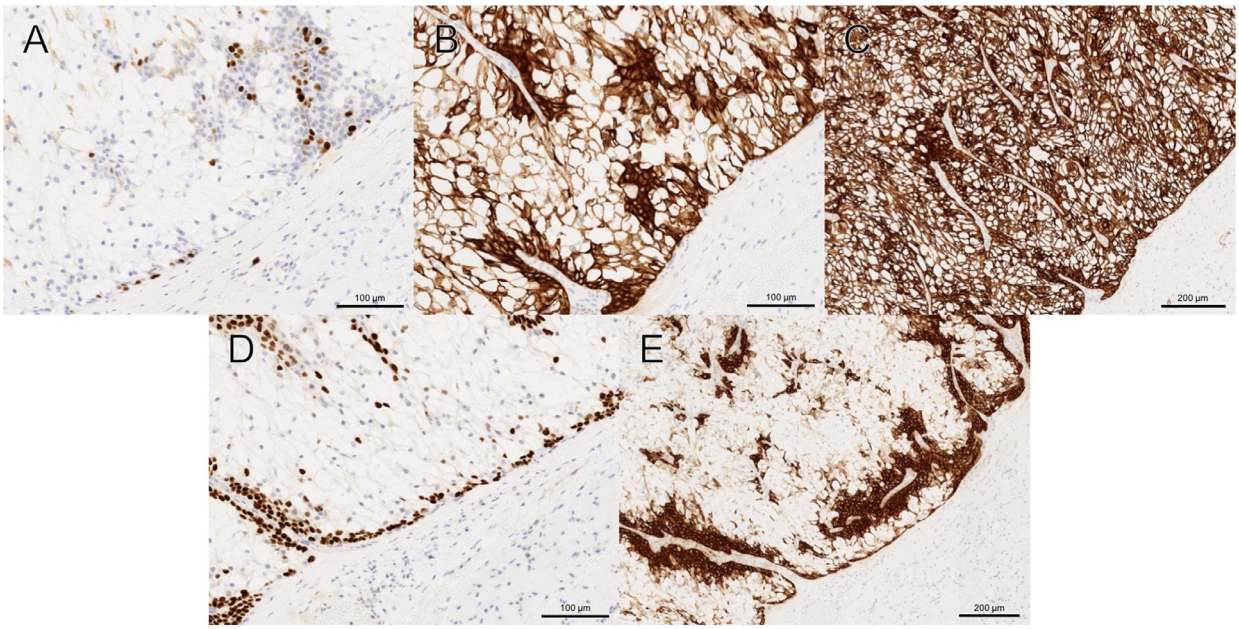

Fig. 2. **(A)** Low MIB1 proliferative index of 2% to 3% mainly within intermediate cell population (MIB1; magnification as illustrated). *A high-resolution version of this slide for use with the Virtual Microscope is available as eSlide: VM05186.* **(B)** 34βE12 demonstrating an intact basal layer with strongly positive intermediate cells and positive clear cells (34βE12; magnification as illustrated). *A high-resolution version of this slide for use with the Virtual Microscope is available as eSlide: VM05201.* **(C)** CK7 showing diffusely positive staining (CK7; magnification as illustrated). *A high-resolution version of this slide for use with the Virtual Microscope is available as eSlide: VM0199.* **(D)** p63 demonstrating intact basal layer (p63; magnification as illustrated). *A high-resolution version of this slide for use with the Virtual Microscope is available as eSlide: VM05191.* **(E)** CK5/6 showing an intact basal layer and positively stained intermediate cells (CK5/6; magnification as illustrated). *A high-resolution version of this slide for use with the Virtual Microscope is available as eSlide: VM05202.*

The final diagnosis was predominately based on morphology and confirmed by the presence of mucinous cells, intermediate cells with cell change, and an intact basal layer verified by immunotyping. CK5/6, directed at myoepithelial cells, confirmed the presence of an intact basal cell layer. Similarly, 34βE12 and SMA stained the cytoplasm of basal cells and aided in the confirmation of an intact basement membrane.

In this case, the initial excisional biopsy specimen was considered representative (no residual lesion) and thus a relatively conservative approach with limited further resectional surgery was favored. In view of complete excision, and in the absence of an invasive component, recurrence was not anticipated.

CONCLUSIONS

Our review of the literature would suggest that this pathology is rare in clinical practice, and because of the lack of specific symptoms and characteristic appearances its clinical diagnosis may be challenging. In common with the previously reported case, this lesion presented clinically as an innocuous-looking submucosal swelling that could otherwise represent a benign salivary mucocele. Clinicians should remain mindful of this rare and unusual pathology in their differential diagnosis.

PRESENTATION

The poster abstract was presented at British Association of Oral and Maxillofacial Surgeons Annual Scientific Meeting, July 22−24, 2015.

REFERENCE

1. Chen KT. Intraductal carcinoma of the oral cavity. *Am J Surg Pathol*. 2005;29:279.

Reprint requests:

Dr Jonathan Bowman,
Department of Oral and Maxillofacial Surgery,
Victoria Hospital,
Kirkcaldy, KY2 5AH,
United Kingdom
jonathanbowman@nhs.net